Circumferential-wave phase velocities for empty, fluid-immersed spherical metal shells

Überall, Herbert; Ahyi, A. C.; Raju, P. K.; Bjørnø, Irina; Jensen, Leif Bjørnø

Published in:
Acoustical Society of America. Journal

Link to article, DOI:
10.1121/1.1512290

Publication date:
2002

Document Version
Publisher's PDF, also known as Version of record

Circumferential-wave phase velocities for empty, fluid-immersed spherical metal shells

Herbert Überall[a)]
Department of Physics, Catholic University of America, Washington, DC 20064

A. Claude Ahyi and P. K. Raju
Department of Mechanical Engineering, Auburn University, Auburn, Alabama 36849-5341

Irina K. Bjørnø[b)] and Leif Bjørnø[b)]
Department of Industrial Acoustics, Technical University of Denmark, DK-2800 Lyngby, Denmark

(Received 29 January 2002; accepted for publication 8 August 2002)

In earlier studies of acoustic scattering resonances and of the dispersive phase velocities of surface waves that generate them [see, e.g., Talmant *et al.*, J. Acoust. Soc. Am. **86**, 278–289 (1989) for spherical aluminum shells] we have demonstrated the effectiveness and accuracy of obtaining phase velocity dispersion curves from the known acoustic resonance frequencies. This possibility is offered through the condition of phase matching after each complete circumnavigation of these waves [Überall *et al.*, J. Acoust. Soc. Am. **61**, 711–715 (1977)], which leads to a very close agreement of resonance results with those calculated from three-dimensional elasticity theory whenever the latter are available. The present investigation is based on the mentioned resonance frequency/elasticity theory connection, and we obtain comparative circumferential-wave dispersion-curve results for water-loaded, evacuated spherical metal shells of aluminum, stainless steel, and tungsten carbide. In particular, the characteristic upturn of the dispersion curves of low-order shell-borne circumferential waves (A or A_0 waves) which takes place on spherical shells when the frequency tends towards very low values, is demonstrated here for all cases of the metals under consideration. © *2002 Acoustical Society of America.* [DOI: 10.1121/1.1512290]

PACS numbers: 43.30.Jx, 43.40.Ey [DEC]

I. INTRODUCTION

Acoustic scattering from bounded objects is often dominated by the associated creation of circumferential waves (surface waves) that can circumnavigate the object along closed paths (great circles on a spherical scatterer, circles or even helical paths on a cylinder, geodesics in general). When returning to their point of origin after each circumnavigation, a ''phase matching condition'' may apply at certain well-defined ''resonance frequencies'' that are determined by the form of the phase velocity vs frequency dispersion curve of these waves. This phase matching leads to a resonant build-up of the circumferential wave that becomes manifest in the scattering process through the radiation of the wave into the ambient field. Such a mechanism has first been pointed out by us quite early,[1] and has subsequently been explored through many specific applications.[2–11]

The circumferential-wave dispersion curves are related to the scattering-resonance frequencies by the formula[1,2] (for the case of spherical scatterers):

$$c/c_w = k_n a(n+\tfrac{1}{2}), \tag{1}$$

where c_w is the sound speed in the ambient fluid (e.g., water), k is the acoustic propagation constant in this fluid, c is the dispersive phase velocity of a circumferential wave, a is the sphere radius, and n is the modal vibration order (which, by phase matching, is the number of circumferential wavelengths spanning the sphere, the term $\frac{1}{2}$ arising from the fact that a quarter-wavelength phase jump takes place as the waves converge at each of the two focal points on the sphere[12]). The corresponding resonance value of k is designated k_n. Equation (1) constitutes the mentioned connection between resonance frequencies k_n and phase-velocity dispersion curves $c(k)$, so that known values of k_n determine the points $c(k_n)$ on the dispersion curves, or vice versa[2] (for cylindrical shells, see Ref. 11).

In Ref. 2, Eq. (1) has been used in order to obtain some limited portions of circumferential-wave dispersion curves for evacuated, water-immersed thin shells of aluminum, stainless steel, and tungsten carbide (WC), based on the calculated resonance frequencies up to $ka=8$ (Al), 3(WC), and 2.3 (steel) that were available at that time. Upturning dispersion curves were found here as ka (i.e., the frequency) tended to lower values (below $ka\cong 3$); this is not the case for cylindrical shells nor for plates[13,14] where the corresponding dispersion curves tend to zero monotonically as the frequency decreases.

The various types of surface waves on shells that are involved here, have dispersion curves that resemble those of the Lamb waves A_0, S_0, A_1, S_1, etc., on a free plate[13–15] when scaled from one to the other object by a formula

$$fh=(c_w/2\pi)ka(1-b/a) \tag{2}$$

due to Dragonette.[16] Here f is the frequency, a is the external shell radius, and b the internal one, and h is the thickness of

[a)]Author to whom correspondence should be addressed. Electronic mail: uberallh@msn.com
[b)]Present address: Stendiget 19, DK2630 Taastrup, Denmark.

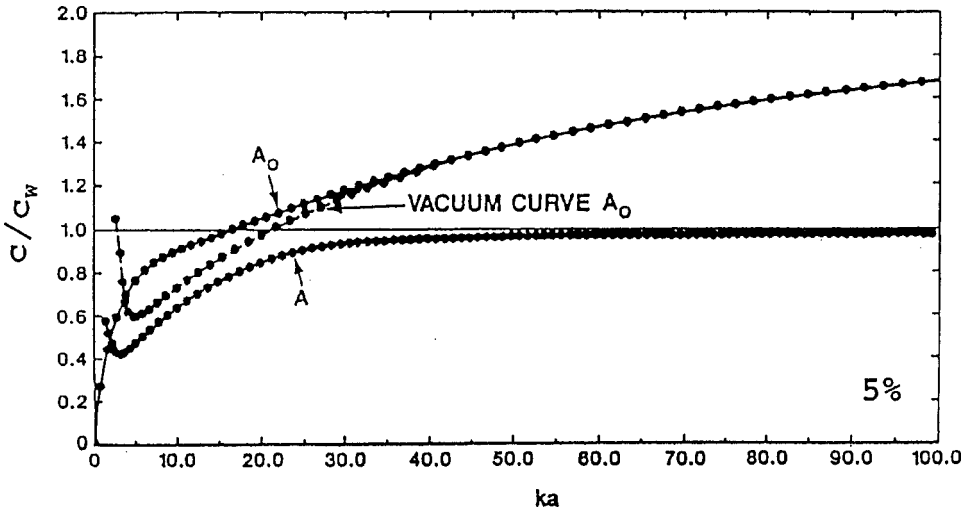

FIG. 1. A_0- and A-wave dispersion curves on a water-loaded, evacuated spherical aluminum shell (5% thick) and A_0 curve for a shell in vacuum. From Refs. 15 and 17 (with permission).

the plate [or, $h \equiv (a-b)$ for the shell]. This resemblance is close for cylindrical shells; for a spherical shell, however, the work of Sammelmann *et al.*[17] has obtained [using three-dimensional (3D)-elasticity theory] phase velocity dispersion curves for aluminum shells that show the mentioned upturn. This is presented here in Fig. 1 in a version adapted[15] from Ref. 17.

Seen in Fig. 1 is, first, the dispersion curve of the A_0 Lamb-type wave for an evacuated aluminum shell in vacuum (designated "vacuum curve A_0"), which shows an upturn at very low values of the dimensionless frequency *ka*. [The thickness indication "5%"of the shell here refers to the value of $(a-b)/a \equiv h/a$]. For the water-loaded, evacuated shell, the A_0 curve now tends toward zero, however. An additional surface wave A (also called[16] a_{0-} and generally referred to as the "Scholte-Stoneley wave"[2,5,6,10]) now appears here, being present due to the water loading of the shell, and it is now the dispersion curve of this A wave that shows the low-frequency upturn. At first thought, the A_0 wave, since existing on the shell with or without fluid loading could be expected to be shell-borne throughout, and the A wave which exists only with the presence of fluid loading could be considered to be fluid-borne throughout (especially since its dispersion curve at $ka \to \infty$ tends towards the sound speed in the ambient fluid). If this were correct, the switch-over of the low-frequency upturn from the A_0 to the A wave upon application of fluid loading would appear to be unexplained.

An explanation for this switch-over phenomenon can be found using a physical argument.[15] The A_0 and the A waves are coupled together (they "interact") by the boundary conditions of the shell-fluid interface. With phase velocities for $f \to \infty$ tending towards the Rayleigh[14] plate-speed (for A_0), and towards c_w (for A), respectively, these limits identify A_0 as being shell-borne, and A as being fluid-borne at large frequencies. With f descending towards the coincidence frequency where $c(A_0)$ approaches c_w, the coupling takes effect, causing the previously converging A_0 and A curves to undergo a "repulsion."[15] During this repulsion the physical nature of the two waves switches around,[18] so that at still lower frequencies (below coincidence), A now is a shell-borne and A_0 a fluid-borne wave. The switch-over of the physical character of modes during curve repulsions as caused by modal coupling is also known in other branches of physics, e.g., in atomic physics.[19]

With this change-over of the nature of the A_0 and A waves, the interpretation of the dispersion curves in Fig. 1 now becomes thus: as low frequencies are approached, it is always the *shell-borne* wave whose dispersion curve shows the upturn, while the dispersion curve of *fluid-borne* wave tends towards zero.

In the following, the generality of this behavior of A_0 and A wave dispersion curves, including their low-frequency upturn, will be demonstrated on the basis of the connection between resonance frequencies and dispersion curves. This will be carried out for water-loaded, evacuated spherical shells of aluminum, stainless steel, and tungsten carbide (WC) of various shell thicknesses. In this way, comprehensive information will be obtained on the quantitative behavior of the corresponding dispersion curves, not previously demonstrated in the literature, for a variety of shell dimensions and suitable for comparisons between shells of different materials.

The approach to be followed here is more general than just being an application to the interacting A_0 and A dispersion curves. As stated, it consists in a comparison of now available calculated dispersion curves with calculated resonance frequency data pertaining to these dispersion curves, in order to show the suitablity of the resonance data for determining the dispersion curves, and the degree of accuracy that can be achieved with this procedure. All this is being carried out here for the A_0 and A-type surface waves, and also for the S_0 wave and even the A_1, S_1, and S_2 waves wherever possible. The shell thickness considered were 1%, 2%, 2.5%, and 5% for aluminum, 1%, 2.3%, and 2.5% for stainless steel, and 1%, 2.5%, and 5% for tungsten carbide (although shells of other thicknesses also are available). As a result, we obtain a comprehensive overview of dispersion curves for the A wave and the lowest Lamb-type waves based on results from calculations and from resonance data, as they are available at present for the mentioned materials; this also allows comparisons between different materials and different shell thickness.

It should be noted that for a given shell material (Al, SS, or WC where SS designates stainless steel), the literature

contains different assumptions about its material parameters. For example, the SS parameters have been taken as $c_L = 5.854 \times 10^5$ cm/s (longitudinal velocity), $c_T = 3.150 \times 10^5$ cm/s (shear velocity) and $\rho = 7.84$ g/cm^3 (density) for 440*c* stainless steel by Ref. 20, or as $c_L = 5.675 \times 10^5$ cm/s, $c_T = 3.141 \times 10^5$ cm/s, and $\rho = 7.57$ g/cm^3 for 304 stainless steel by Ref. 3. It has been found, however,[3] that, e.g., the *A*-wave amplitude is only very wealy dependent on the material parameters and the shell thickness. We may assume, therefore, that dispersion and resonance data obtained using material parameters differing from each other by only the small amounts illustrated above, may be used interchangeable in the following for our comparison purposes. If necessary, a curvature correction due to Marston[21] may be applied in order to convert dispersion curves valid for a plate to those for a shell of given radius and thickness; such results are illustrate for 16.2% steel shells[20] and are significant for substantial shell thicknesses only.

II. ALUMINUM SHELLS

Application of the phase matching procedure which furnishes the resonance/dispersion curve connection has been initiated by Talmant *et al.*[2] for the case of spherical aluminum shells. In this reference, the Scholte-Stoneley wave (called the *A* wave) has first been identified on spherical shells, simultaneously with the work of Sammelmann *et al.*[17] where it was called the a_0-wave), see Fig. 1. To illustrate this connection, Fig. 2(a) shows the calculated resonances in the far-field backscattering amplitude (or from function) plotted vs ka ($k = \omega/c_w$, a=outer shell radius) for an air-filled aluminum shell in water, of thickness 5%, and Fig. 2(b) shows the *A*-wave dispersion curve for this aluminum shell (or rather, the resonance points thereof) obtained from Eq. (1). This curve displays the low-flow-frequency upturn of the *A*-wave curve that was mentioned earlier. Also shown in Fig. 2(b) are portions of the *A*-wave dispersion curves for 1% steel and 1% WC shells as they have been available in Ref. 2, and which shall be discussed below. These portions belong solely to the upturning regions of the corresponding dispersion curves.

A very instructive picture of the calculated resonance response (i.e., of the form function after coherent subtraction of the specular reflection amplitude) is given in Fig. 3 for a 2.5% shell (from Ref. 2), which distinguishes between the resonances of the *A* wave and those of the S_0 wave with their mode orders *n* as indicated. Further, more extended resonance graphs are given in the same reference. These will be used here for establishing the resonance/dispersion curve connection for aluminum shells.

Calculated dispersion curves are shown in Fig. 1, or are contained in several figures of Ref. 2 for the *A* and A_0 waves. For obtaining further Lamb mode dispersion curves, it is possible to use the values for a one-sided water-loaded plate,[13] or even for a free plate[15] as stated in Ref. 6; as a matter of fact, the agreement of the resonance value predictions with the free-plate dispersion curves as shown in the following figures (e.g., for the S_0 wave) is a demonstration of the validity of such a procedure. The frequency scale for plates, usually given by the variable fd (in units mm/μs

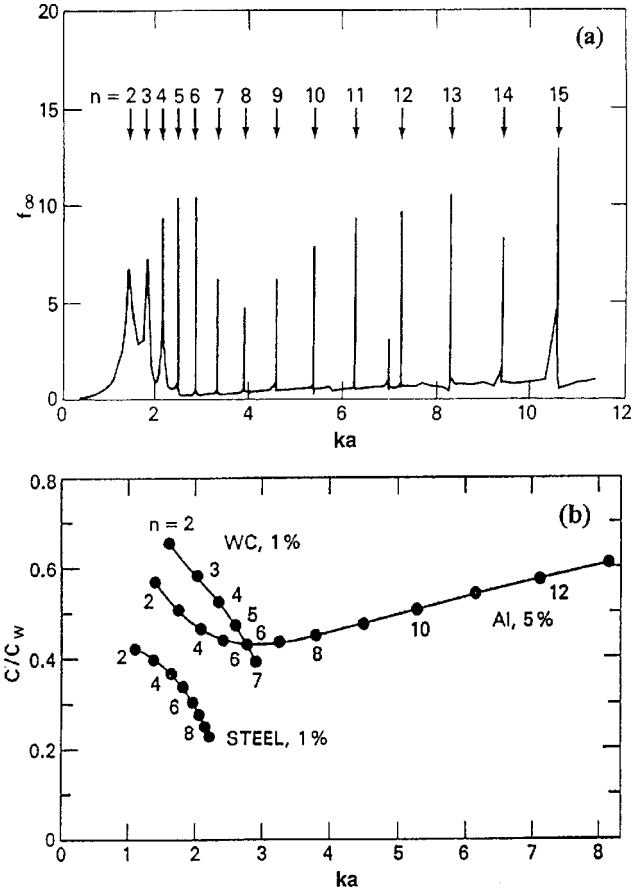

FIG. 2. (a) Resonances in the form function (≡far field backscattering amplitude) of an air-filled aluminum shell in water, of thickness 5%, plotted vs *ka*. (b) Dispersion curve of the *A* wave on the aluminum shell, plotted vs *ka*. Also shown are portions of the dispersion curves for 1% steel and 1% WC shells. From Ref. 2.

where *d* is the plate thickness) is related by Eq. (2) (where the plate thickness was called *h*) to the *ka* scale for shells. Figure 4 shows this *fd* scale and simultaneously the *ka* scales for 1%, 2.5%, and 5% shells, the curves thus being in a sense universal for all shell thickness (it should be kept in mind that this applies to thin shells only). Note that a conversion of the dispersion curves for a shell of one thickness to the plate scale by the Dragonette formula Eq. (2), with a subsequent reconversion to a shell of different thickness, allows to convert dispersion curves from a shell of one thickness to those of a different thickness, as we shall occasionally do below.

Figure 4 shows our results for the *A*, A_0, and S_0 wave dispersion curves of an aluminum shell. The calculated dispersion curves labeled A_0, $A^{\text{vac}}_{0,\text{sph}}$ are obtained from the 5%-shell curves of Fig. 1, and those labeled $A^{\text{vac}}_{0,\text{pl}}$, $S^{\text{vac}}_{0,\text{pl}}$, and $A^{\text{vac}}_{1,\text{pl}}$ (the free-plate curves) from Ref. 2 or 15. The cutoff frequency of $A^{\text{vac}}_{1,\text{pl}}$ is obtained from Brekhovskikh,[22] and it is known that the A_1, S_1, etc., curves for $f \to \infty$ tend towards the shear speed c_T in the plate material while those of the A_0 and S_0 wave tends towards[14] the Raleigh speed c_R as indicated; the *A*-wave speed tends toward the sound speed in water, c_w. The aluminum parameters were here assumed[2] as $c_L = 6350$ m/s, $c_s = 3050$ m/s, and $\rho = 2.7$ g/cm^3, differing only insignificantly from those of Ref. 15. The (selected)

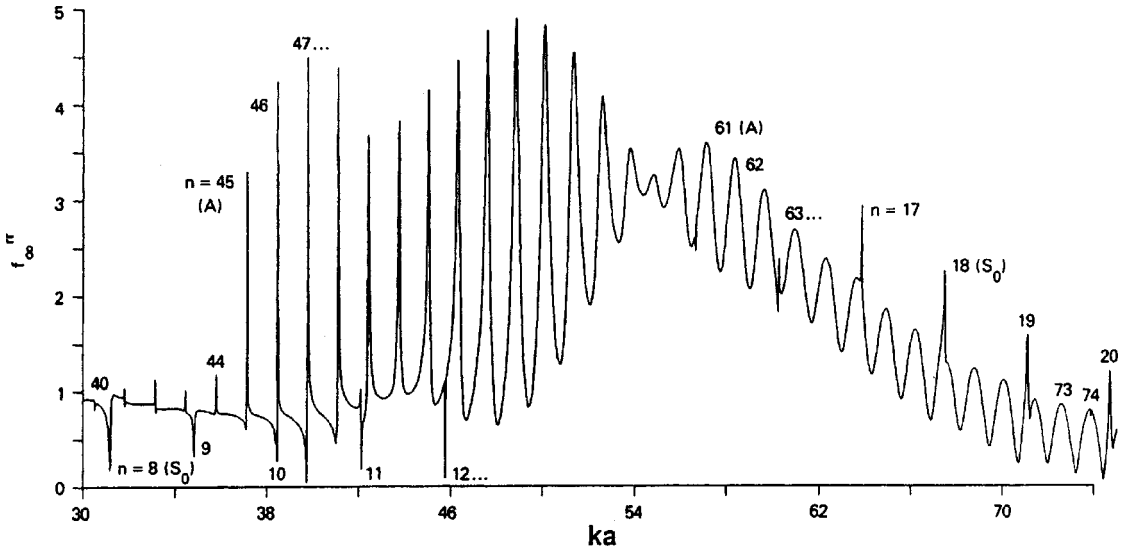

FIG. 3. Resonance response of a 2.5% Al shell plotted vs *ka*. From Ref. 2.

resonance points in Fig. 4, labeled by their numbers *n*, are found from the resonance frequency values of Ref. 2, Figs. 1, 2, 10, and 12. The agreement is perfect, even for the S_0 wave where the resonance values are compared to the plate-wave dispersion curve.

Figure 5 shows the A_0 and A wave results of Fig. 4 on an enlarged scale, and Fig. 6 those of the A wave, further enlarged, for the 5% shell and with the calculated 2% shell dispersion curves added on either the 2% scale or on the 5% scale. The results presented here illustrate the power of the resonance/dispersion curve comparisons, and demonstrate the agreement between the two approaches for the A, A_0, and S_0, waves in thin aluminum shells of various thickness. Similar results will now be shown for shells of stainless steel and of tungsten carbide.

III. STAINLESS STEEL SHELLS

For the case of evacuated, water-immersed stainless steel shells there exist previous calculations of both surface-wave dispersion curves,[3,4,20,24] and of the resonances caused by them.[23–26] These will be useful for the present study in which resonance results will be superimposed with the dispersion curves.

The calculated dispersion curves in Fig. 2 of Ref. 3 for the A_0 and A waves of a stainless steel shell are the analogs of our present Fig. 1 for the aluminum shell. They refer to a 2.3% SS 304 empty spherical shell immersed in water. Since we will use these resulting curves to compare with the resonances of a 2.5% thick spherical shell, we can readjust the curves to the 2.5% scale by employing Dragonette's formula Eq. (2) twice. In addition, we may rescale in the variable *ka*, as indicated, e.g., in Fig. 4, to other shell thicknesses, e.g., to a 5% shell.

For that latter case, we present our comparisons in Fig. 5(a) where the solid dispersion curves are those of Ref. 3 (re-scaled as mentioned) for the A_0 and A waves, and that for the S_0 wave is from Ref. 20 which also shows A_1 and S_1 curves. The upturn of this latter curve for low frequencies was found[20] to be eliminated (rendered horizontal) by Marston's curvature correction;[21] both versions are indicated here. For the Lamb wave curves, we used those for a free plate. Here, the A_1, S_1, and S_2 waves are included, and their low-frequency cutoff values were obtained from the formulas of Brehovshikh.[22]

The resonance-generated curve points come from the calculated resonance values of Ref. 24, marked by their mode numbers *n*. As to the agreement of the A_1 and S_1 resonance points with the dispersion curves for plates that were employed here, this is by and large satisfactory, with the more important deviations occurring in the right direction predicted by Marston's curvature corrections as illustrated in Fig. A2 of Ref. 20.

The A_0 and A wave results form a crucial part of Fig. 5(a), for which the Kaduchak–Marston curves[3] provided the same clarification for the stainless steel shells that the results of Sammelmann *et al.*[17] (reproduced in our Fig. 1) did for the aluminum shells; we shall elaborate on this in the following portions of Fig. 5 below. The Lamb-wave parts in Fig. 5(a) have the same layout as in Fig. 4 of Ref. 24; however, the A_0 and A parts in that latter reference are incomplete insofar as they only present limited portions of the two curves one at a time not indicated by their labeling. The reason for this is that calculated resonance response of the steel shell in Ref. 24 (the analog to our Fig. 3 for Al) does not show all the resonances present, with the S_0 and A wave resonances clearly visible but those of the A_0 wave totally obscured due to their overlapping widths (thus forming just one broad hump in Fig. 3, referred to as the ''midfrequency enhancement'' by Marston *et al.*[3]). The visible A-wave resonances become increasingly narrow in the low-frequency region, but have nevertheless been calculated in an approach effective for ultranarrow resonances by Ref. 23. In Fig. 5(c) the calculated A_0 and A wave dispersion curves are shown correctly (as well as that for the A_0 wave for a shell in vacuum) but only on a smaller scale; in the following Fig. 5(b) we increase this scale and add the resonance results.

The low frequency upturn of the A (or A_0^{vacuum}) curves seen for Al in Fig. 1 is also present for SS shells, cf. Figs.

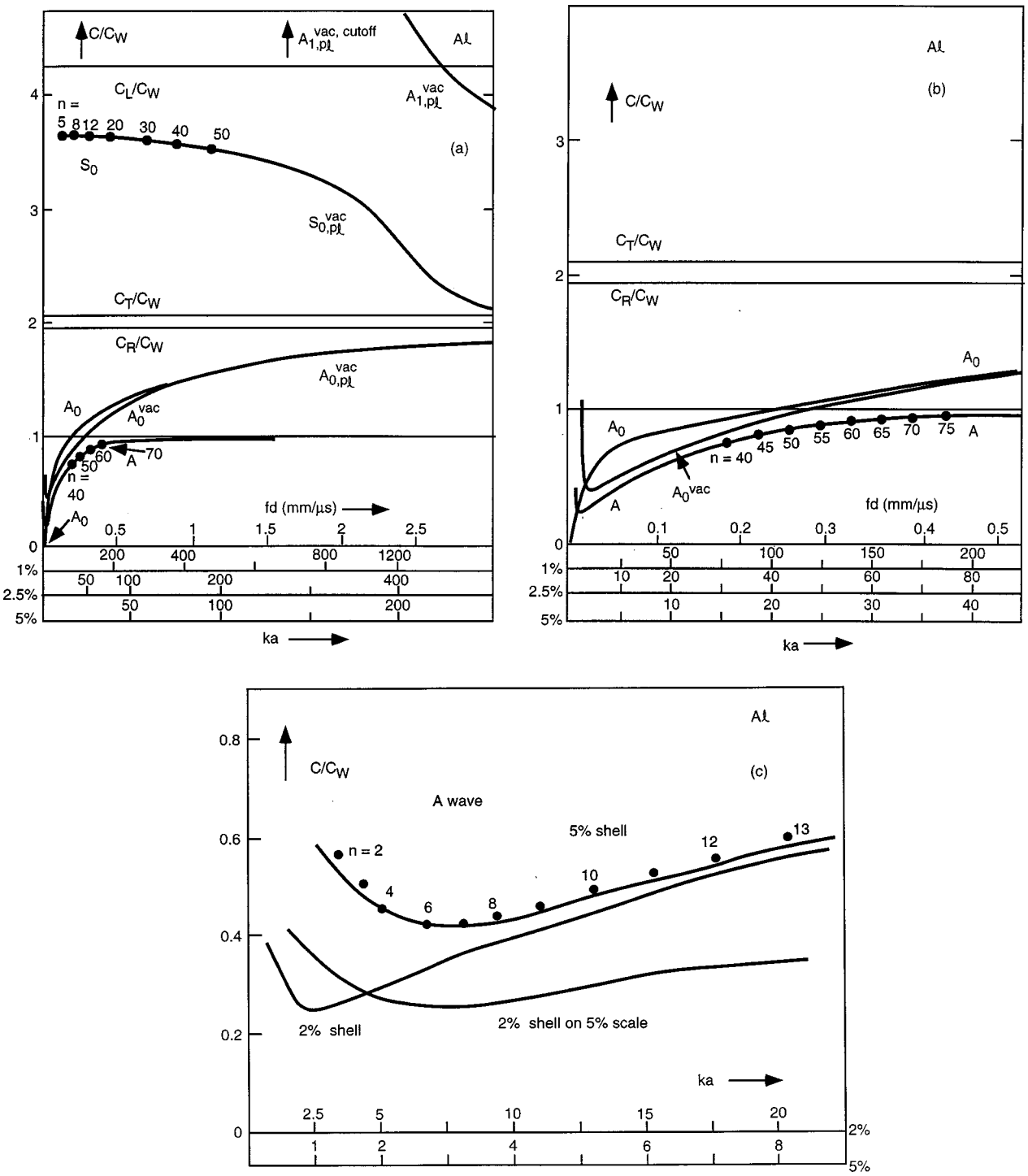

FIG. 4. Comparison of calculated dispersion curves on water-loaded, evacuated spherical aluminum shells with results obtained from calculated resonance frequencies (5% thickness); (a) for A, A_0, and S_0 waves (A_1 wave also indicated); (b) for A and A_0 waves on an extended scale; (c) for the A wave, further extended scale and 2% shell curve added.

4(b) and (c). It is interesting to note, however, that this upturn does not proceed to infinity but that at even lower frequencies, it goes through a maximum and is followed by a downturn, so that the A curve finally ends up at zero for $f \rightarrow 0$ as shown in Ref. 4.

The low-frequency portions of the dispersion curves of Fig. 5(a) are plotted on a larger scale in Fig. 5(b). The calculated A_0, A_0^{vac}, and A wave dispersion curves for 2.5% steel shells are entered following Kaduchak and Marston,[3] except that their A-wave curve is extended to lower frequencies, drawn through the resonance points to guide the eye. The resonance points originate with Marston and Sun[23] (2.5% shells, open circles), with Ref. 25 (2.5% and 1% shells, crosses), and with Ref. 2 (1% shells, solid circles). These latter points were first obtained by Junger,[27] constituting his "lower ($j=1$) branch" of spherical shell vibrations, and may be referred to as the resonances of the "Junger wave."

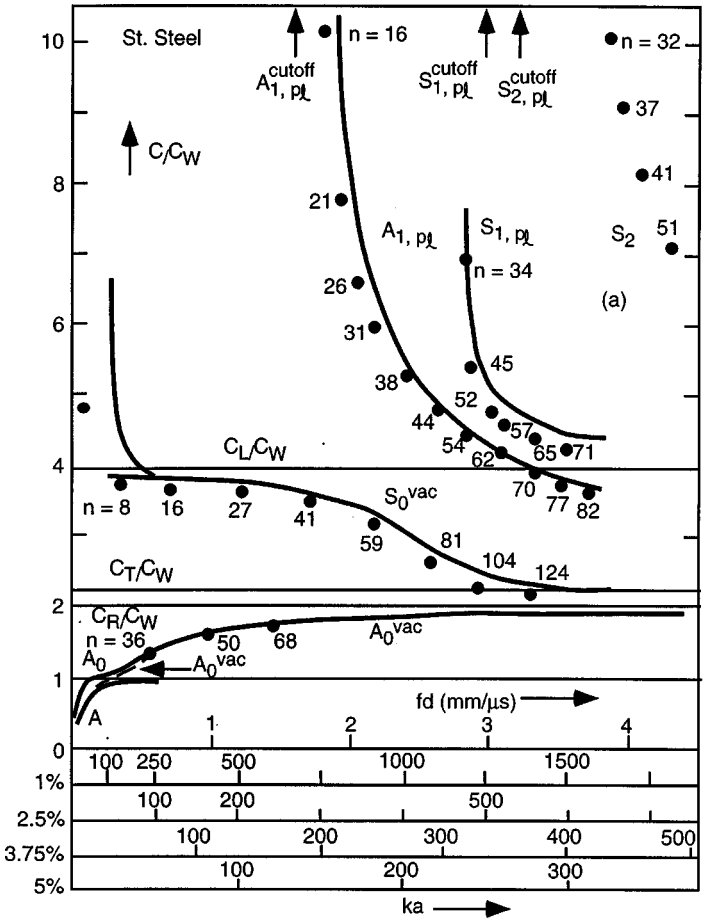

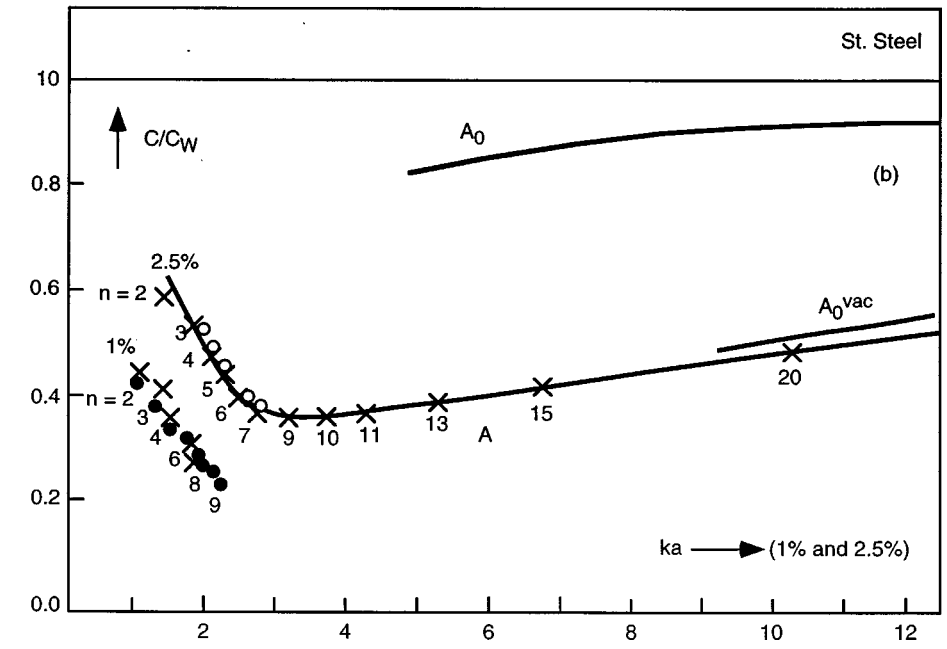

FIG. 5. Comparison of calculated dispersion curves on water-loaded, evacuated spherical stainless steel shells with results obtained from calculated resonance frequencies: (a) for A, A_0, S_0, A_1, and S_1 waves (S_2 wave also indicated), 5% thickness; (b) for A and A_0 waves at 2.5% thick shells (1% resonance points added).

The results for the 2.5% steel shell as shown here demonstrate the low-frequency upturn of the A wave, as noted earlier for the Al shell; cf., e.g., Fig. 4(c). By comparison with the 5% and 2% A curves for Al, Fig. 5(b) shows analogous 2.5% and 1% A curves for steel, and by this analogy, it becomes clear that the Junger wave on a 1% steel shell is the low-frequency upturning extension of the A-wave dispersion curve of the water-loaded shell.[28]

IV. TUNGSTEN CARBIDE SHELLS

For the case of evacuated tungsten carbide (WC) shells immersed in water, the literature contains calculated dispersion curves for 1% and 2.5% shell thicknesses,[2] as well as a calculated resonance spectrum for a 1% shell [Fig. 3(a) of Ref. 2]. For that calculation, we assumed WC material parameters $\rho = 13.80$ g/cm^3, $c_L = 6.860 \times 10^5$ cm/s, and c_T

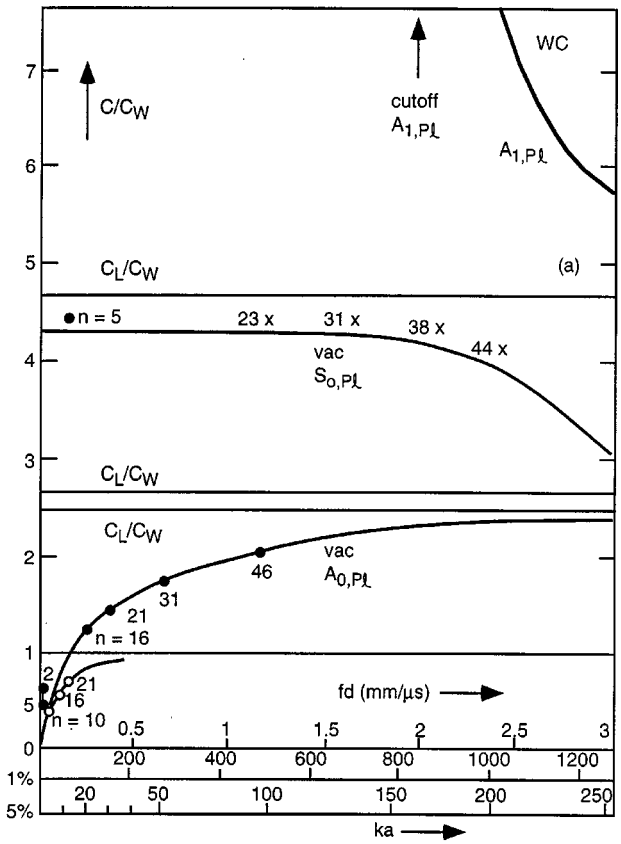

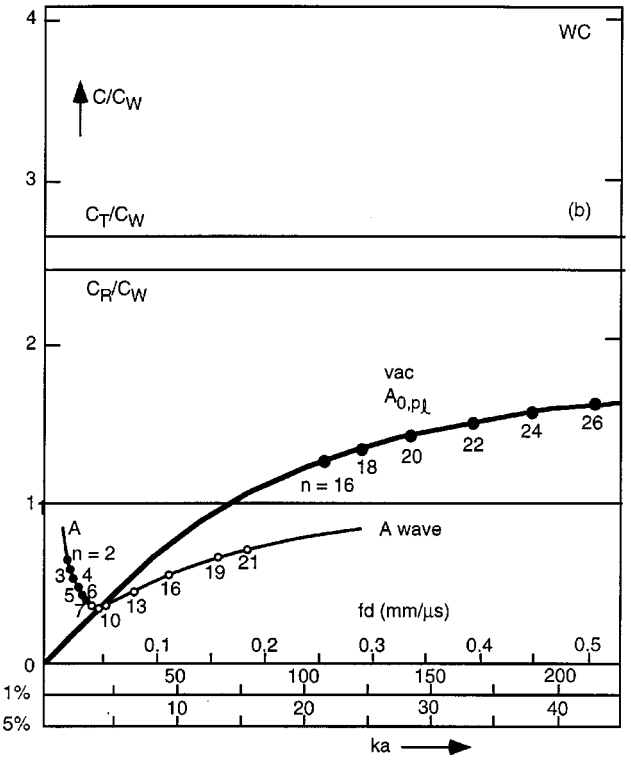

FIG. 6. Comparison of calculated dispersion curves on water-loaded, evacuated spherical tungsten-carbide shells with results obtained from calculated resonance frequencies: (a) for A, A_0, and S_0 waves (A_1 wave also indicated); (b) for A and A_0 waves at 1% shell thickness.

$=4.185\times10^5$ cm/s; for water $\rho_w=1$ g/cm^3 and $c_w=1.4825$ km/s. Low-frequency resonances were calculated for a 1% shell, and the resulting resonance points of the A wave were entered in the present Fig. 2(b). While Ref. 29 contains calculated resonances for 1% and 5% shells, only the dispersion curves for WC plates are exhibited in this reference. The resonances are shown here in the fashion of the present Fig. 3, and are analyzed only for the S_0 and A_0 wave resonances. However, the A-wave resonances are also visible in Figs. 2 and 3 of Ref. 29, and are here extracted by us for the purposes of the present study.

Our results are shown in Fig. 6. Here, Fig. 6(a) which is patterned after Fig. 4(a) for Al and Fig. 5(a) for SS, exhibits the dispersion curves of the Lamb waves A_0, and S_0, and A_1 for plates, as well as of the A wave with its characteristic low-frequency upturn; resonance points from Refs. 2 and 29 have also been entered, indicating their mode numbers n. As we did before, only selected resonance points are entered in our figures, sufficient to assess their agreement with the calculated curves.

The low-frequency behavior of the A and A_0 waves is visible in the lower left corner of Fig. 6(a), but is shown in detail in Fig. 6(b) on an extended scale. The A_0-wave points of $n=16,18,\ldots$ and the A-wave points $n=8,9,10,13,\ldots$ come from Fig. 2 or 3 of Ref. 29 which, as stated, are amenable to having their resonances interpreted in terms of these waves. The resonance points $n=2-7$ are those of Fig. 2(b), stemming from Ref. 2; the resulting curve joins smoothly with that through the $n\geqslant 8$ points and legitimizes their interpretation in terms of the A-wave curve with its familiar low-frequency upturn.

V. SUMMARY AND CONCLUSIONS

The present study constitutes an overview of the dispersion curves for the Lamb waves A_0, S_0, A_1, S_1, etc., and for the Scholte-Stoneley A wave on thin, water-immersed and evacuated (or, alternately, the closely similar air-filled) spherical shells of aluminum, stainless steel, and tungsten carbide. This study is based on all the information available in the literature for these shells, regarding the dispersion curves for A, A_0, S_0, etc., waves, as well as the resonance frequencies generated by the phase matching during circumferential propagation of these waves around the shells. The resonance frequencies have been used to obtain individual points on the dispersion curves, enabling us to judge their fits with the calculated continuous dispersion curves. Our Figs. 4, 5, and 6 form the gist of our present study.

Of special interest here is the clarification of the low-frequency behavior of the interacting dispersion curves of the A and A_0 waves, which the previous literature showed to be known only in a tentative, or even ill-understood fashion. For all three shell materials considered here, the clarifying picture of calculated dispersion curves for Al of Fig. 1 (due to Sammelmann *et al.*[17]), as well as the corresponding clarification for SS due to Kaduchak and Marston,[3] has been conformed by the fits of the resonance points superimposed on these curves. The same has been shown here to hold for WC shells, so that the low-frequency upturn of the A-wave dispersion curve, together with the progression to zero of the A_0-wave curve, is now recognized as a quite universal phenomenon. We believe that our present overview of the Lamb and Scholte-Stoneley wave behavior (regarding dispersion curves and resonance frequencies) for thin spherical shells

with the different shell materials considered here constitutes a comprehensive picture of the physical phenomena involved, that had been presented in the previous literature only in a disjoint, and sometimes only partially understood, fashion.

ACKNOWLEDGMENTS

One of the authors (H.Ü.) acknowledges the hospitality of Professor P. K. Raju and Professor L. Bjørnø at their respective institutions.

[1] H. Überall, L. R. Dragonette, and L. Flax, "Relation between creeping waves and normal modes of vibration of a curved body," J. Acoust. Soc. Am. **61**, 711–715 (1977).
[2] M. Talmant, H. Überall, R. D. Miller, M. F. Werby, and J. W. Dickey, "Lamb waves and fluid-borne waves on water-loaded, air-filled thin spherical shells," J. Acoust. Soc. Am. **86**, 278–289 (1989).
[3] G. Kaduchak and P. L. Marston, "Observation of the midfrequency enhancement of tone bursts backscattered by a thin spherical shell in water near the coincidence frequency," J. Acoust. Soc. Am. **96**, 224–230 (1993).
[4] G. Kaduchak, C. S. Kwiatkowski, and P. L. Marston, "Measurement and interpretation of the impulse response for backscattering by a thin spherical shell using a broad-bandwidth source that is nearly acoustically transparent," J. Acoust. Soc. Am. **97**, 2699–2708 (1995).
[5] G. Maze, F. Léon, J. Ripoche, A. Klauson, J. Metsaveer, and H. Überall, "Nature de l'onde d'interface de Scholte sur une coque cylindrique," Acustica **81**, 201–213 (1995).
[6] H. Überall, A. Gérard, A. Guran, J. Duclos, M. Khelil, X. L. Bao, and P. K. Raju, "Acoustical scattering resonances: relation to external and internal surface waves," Appl. Mech. Rev. **49**, S63–S71 (1996).
[7] J. P. Sessarego, J. Sageloli, R. Guillermin, and H. Überall, "Scattering by an elastic sphere embedded in an elastic isotropic medium," J. Acoust. Soc. Am. **104**, 2836–2844 (1998).
[8] A. C. Ahyi, P. Pernod, O. Gatti, V. Latard, A. Merlen, and H. Überall, "Experimental demonstration of the pseudo-Rayleigh (A_0) wave," J. Acoust. Soc. Am. **104**, 2727–2732 (1998).
[9] X. L. Bao, P. K. Raju, and H. Überall, "Circumferential waves on an immersed, fluid-filled elastic cylindrical shell," J. Acoust. Soc. Am. **105**, 2704–2709 (1999).
[10] H. Überall, "Acoustic of a shell," Acoustical Physics **47**, 115-139 (2001), translated from Russian [Akusticheskii Zhurnal **47**, 149–177 (2001)].
[11] X. L. Bao, H. Überall, P. K. Raju, A. C. Ahyi, I. K. Bjørnø and L. Bjørnø, "Waves on fluid-loaded shells and their resonance frequency spectrum," preprint.
[12] See, e.g., A. Sommerfeld, *Optics* (Dover, New York, 1945).
[13] X. L. Bao, H. Franklin, P. K. Raju, and H. Überall, "The splitting of dispersion curves for plates fluid-loaded on both sides," J. Acoust. Soc. Am. **102**, 1246–1248 (1997).
[14] M. F. Werby and H. Überall, "The analysis and interpretation of some special properties of higher-order symmetric Lamb waves: The case for plates," J. Acoust. Soc. Am. **111**, 2686–2691 (2002). See also M. F. Werby and H. Überall, "A systematic study of water-filled, submerged elastic spherical shells and the resolution of elastic and water-included resources," J. Acoust. Soc. Am. **112**, 896–905 (2002).
[15] H. Überall, B. Hosten, M. Deschamps, and A. Gérard, "Repulsion of phase velocity dispersion curves and the nature of plate vibrations," J. Acoust. Soc. Am. **96**, 908–917 (1994).
[16] L. R. Dragonette, Ph.D. thesis, The Catholic University of America, Washington, DC, 1978; also NRL Report 8216, Naval Research Laboratory, Washington, DC, 1978.
[17] G. S. Sammelmann, D. H. Trivett, and R. H. Hackman, "The acoustic scattering by a submerged spherical shell I," J. Acoust. Soc. Am. **85**, 114–124 (1989).
[18] M. Talmant, G. Quentin, J. L. Rousselot, J. V. Subrahmanyam, and H. Überall, "Acoustic resonances of thin cylindrical shells and the resonance scattering theory," J. Acoust. Soc. Am. **84**, 681–688 (1988).
[19] See, e.g., P. H. E. Meijer and E. Bauer, *Group Theory* (North-Holland, Amsterdam, 1965), p. 52.
[20] S. G. Kargl and P. L. Marston, "Ray synthesis of Lamb wave contributions to the total scattering cross section for an elastic spherical shell," J. Acoust. Soc. Am. **88**, 1103–1113 (1990).
[21] P. L. Marston, "Phase velocity of Lamb waves on a spherical shell: Approximate dependence on curvature from kinematics," J. Acoust. Soc. Am. **85**, 2663–2665 (1989).
[22] L. Brekhovskikh, *Waves in Layered Media*, 1st ed. (Academic, New York, 1960), Chap. 1.
[23] P. L. Marston and N. H. Sun, "Resonance and interference scattering near the coincidence frequency of a thin spherical shell. An approximate ray synthesis," J. Acoust. Soc. Am. **92**, 3315–3319 (1992).
[24] G. C. Gaunaurd and M. F. Werby, "Lamb and creeping waves around submerged spherical shells resonantly excited by sound scattering II: Further applications," J. Acoust. Soc. Am. **89**, 1656–1667 (1991).
[25] H. C. Strifors and G. C. Gaunaurd, "Multipole character of the large-amplitude, low-frequency resonances in the sonar echoes of submerged spherical shells," Int. J. Solids Struct. **29**, 121–130 (1992).
[26] G. C. Gaunaurd and M. F. Werby, "Sound scattering by resonantly excited, fluid-loaded elastic spherical shells," J. Acoust. Soc. Am. **90**, 2536–2550 (1991).
[27] M. C. Junger, "Normal modes of submerged plates and shells," in *Fluid–Solid Interaction*, edited by J. E. Greenspan (Proc. ASME Colloquium, New York, 1967), p. 95.
[28] H. Überall, I. K. Bjørnø, and L. Bjørnø, "Dispersion of circumferential waves on evacuated, water-loaded spherical steel shells," Ultrasonics **37**, 673–675 (2000).
[29] V. M. Ayres, G. C. Gaunaurd, C. Y. Tsui, and M. F. Werby, "The effects of Lamb waves on the sonar cross-sections of elastic spherical shells," Int. J. Solids Struct. **23**, 937–946 (1987).